

Cite this article: C.S. Verma, N. Shukla, P. Bose, Study of surface morphology and elemental investigation of chemically deposited mixed based photoconducting ( $Cd_x-Pb_y-Zn_z$ )S films, *RP Materials: Proceedings* Vol. 3, Part 1 (2024) pp. 1–6.

## Original Research Article

# Study of surface morphology and elemental investigation of chemically deposited mixed based photoconducting ( $Cd_x-Pb_y-Zn_z$ )S films

Chandra Shekhar Verma<sup>1,\*</sup>, Neelam Shukla<sup>2</sup>, Purna Bose<sup>1</sup>

<sup>1</sup>Department of Physics, Govt. V.Y.T.P.G. Autonomous College, Durg (C.G.), India

<sup>2</sup>Department of Physics, Kalyan P.G. College, Bhilai, Durg (C.G.), India

\*Corresponding author, E-mail: [shekhar090677@gmail.com](mailto:shekhar090677@gmail.com)

\*\*Selection and Peer-Review under responsibility of the Scientific Committee of the 2<sup>nd</sup> International Conference on Recent Trends in Materials Science & Devices 2023 (ICRTMD 2023).

### ARTICLE HISTORY

Received: 18 Dec. 2023

Revised: 27 Jan. 2024

Accepted: 28 Jan. 2024

Published online: 29 Jan. 2024

### KEYWORDS

Chemical bath deposition technique; XRD; SEM; EDAX; FTIR.

### ABSTRACT

( $Cd_x-Pb_y-Zn_z$ )S thin films have been deposited on glass substrates by cost-effective and very simple method called chemical bath deposition technique at 60°C in an aqueous ammonium solution of bath containing cadmium acetate, zinc acetate, lead acetate and thiourea using double distilled water at different concentration for their potential application in optoelectronic devices. X-ray diffraction (XRD) spectra revealed the structural properties of the films that deposited thin films exhibit both cubic and hexagonal crystal structure. Scanning electron microscope (SEM) Study for the Surface morphology of the as deposited films confirm that the cabbage type structure present in the sample and elemental study using Energy-dispersive X-ray analysis (EDAX) were done and it is confirm that all the elements used to prepared films are present. The Fourier transform infrared (FTIR) spectra show different chemical bonds present in the as-deposited film.

## 1. Introduction

The electro-optical properties of binary and ternary ZnS/CdS/PbS/(Cd-Pb)S/(Cd-Zn)S thin films prepared by the CBD technique have piqued the interest of researchers because this technique is regarded as one of the simplest and most cost-effective methods for producing high-quality nano-crystalline films. Photoconductors are normally composed of semiconductors, which show an enhancement in electrical conductivity due to the absorption of photons. Among the binary compounds, PbS, ZnS, and CdS are the most typical inorganic semiconductor materials owing to their band structure. The properties of (Cd-Zn)S and (Cd-Pb)S thin films lie between the properties of CdS, PbS, and ZnS, widely used as a wide band gap window material in heterojunction photovoltaic solar cells and in photoconductive devices [1].

Ternary films based on CdS, PbS, and ZnS have a percentage of ( $Cd_xPb_{1-x}S$ )/( $Cd_xZn_{1-x}S$ ), and optical investigations demonstrate that the band gap value of these ternary compounds varies with x. The current investigation addresses the generation and surface characteristics of thin films composed of quaternary metal sulfide ( $Cd_x-Pb_y-Zn_z$ )S on glass substrates adopting the CBD technique.

## 2. Materials and methods

### 2.1 Materials

The thin films ( $Cd_x-Pb_y-Zn_z$ )S were deposited using cadmium acetate  $Cd[(C_2H_3O_2)_2 \cdot 2H_2O]$ , zinc acetate  $Zn[(C_2H_3O_2)_2 \cdot 2H_2O]$ , lead acetate  $Pb[(C_2H_3O_2)_2 \cdot 2H_2O]$ , and thiourea  $[NH_2-CS-NH_2]$  of 1M solution as a source of ions for  $Cd^{2+}$  [2]. An aqueous ammonia solution 30% was utilized to

keep the pH level at 11, and tri ethanolamine was employed as a complexing agent. At low temperatures, this solution controls the chemical reaction, and prevents the creation of colloids in solution; at high temperatures,  $NH_3$  evaporates as a HO<sup>-</sup> ion, and film growth gets controlled by cluster-by-cluster mechanisms [2]. The beaker containing the aqueous solution of the chemicals is well covered with another inverted, larger beaker to prevent some ammonia loss. The solution is stirred for a few minutes during its beginning, and no further stirring is done during the deposition. The concentration of the precursor solution for cadmium acetate, zinc acetate, lead acetate, and thiourea was 1M for each solution. After being removed from the chemical bath, the formed thin films were washed with de-ionized water to collect loosely adhered particles on the substrate surface [3].

### 2.2 Methods

The films are deposited utilizing chemical bath deposition techniques. This method of production is one of the most inexpensive and easy-to-follow methods for synthesizing mixed-base ( $Cd_x-Pb_y-Zn_z$ )S type films. Several techniques, such as thermal evaporation, RF sputtering, pulsed laser evaporation, chemical vapor deposition (CVD), and chemical bath deposition (CBD), have been used for forming ( $Cd_x-Pb_y-Zn_z$ )S thin films. Chemical bath deposition is the most advantageous of these procedures since it is inexpensive and can be used to produce thin coatings over a vast area. The surface of ( $Cd_x-Pb_y-Zn_z$ )S thin films produced by chemical bath deposition is typically observed to be smooth and layered.



The As-deposited  $(\text{Cd}_x\text{-Pb}_y\text{-Zn}_z)\text{S}$  thin films were left for 24 hours at room temperature for drying in a desiccator. The structural analysis of thin films was carried out by an X-ray diffractometer using  $\text{Cu-K}\alpha$  radiation ( $\lambda = 1.5405 \text{ \AA}$ ) [4]. A scanning electron microscope (SEM) equipped with an energy-dispersive analysis of X-rays (EDAX) was implemented to analyse the microstructure and elemental composition of the thin films. The Fourier transform infrared spectra for thin films deposited were recorded.

### 2.3 Characterizations

#### 2.3.1 Photoconductivity study

For the PC and DC study tests [5], the photo excitation source was a commercial 100W incandescent bulb, and the voltage source was a regulated power supply. The film's responses were identified by monitoring photocurrent with respect to time and voltage [6]. The entrapment and recombination centres that have been discovered inside the material are well known to influence the rising and fading photocurrent curves. These curves could help us understand the nature and occurrence of trapping and recombination centres. Photoconductive materials' reaction time is an important feature. Response times are slow when there are several trapping centres. When the excitation source is removed, the carriers are gradually released; hence, trapping increases the decay time. Thin film photoconductive properties have been widely investigated for a number of reasons [7].

**Study of photocurrent:** Different concentrations for the system's  $(\text{Cd}_x\text{-Pb}_y\text{-Zn}_z)\text{S}$  photoconductivity were demonstrated for samples S-1, S-2, S-3, and S-4. According to Figure 1 photocurrent ranges from  $2.0 \times 10^{-6} \text{ A}$  to  $4.75 \times 10^{-6} \text{ A}$ , with the maximum being  $4.75 \times 10^{-6} \text{ A}$  for sample number 3. As PC gain ranges from  $6.6 \times 10^5$  to  $47.5 \times 10^6$ , the maximum gain obtained was  $47.5 \times 10^6$ . This graph depicts the development and degradation of photocurrent in materials deposited at various concentrations. In this image, it is obvious that photocurrent influences concentrations of the produced sample and is greatest for sample No. 3 [8].

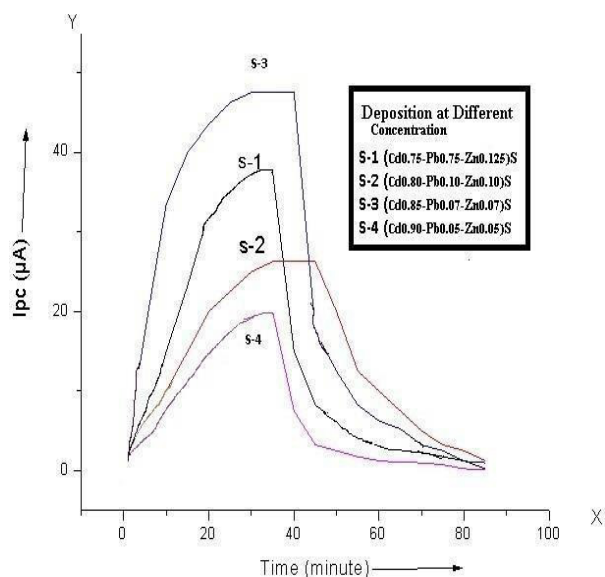


Figure 1: Photocurrent v/s Time [1].

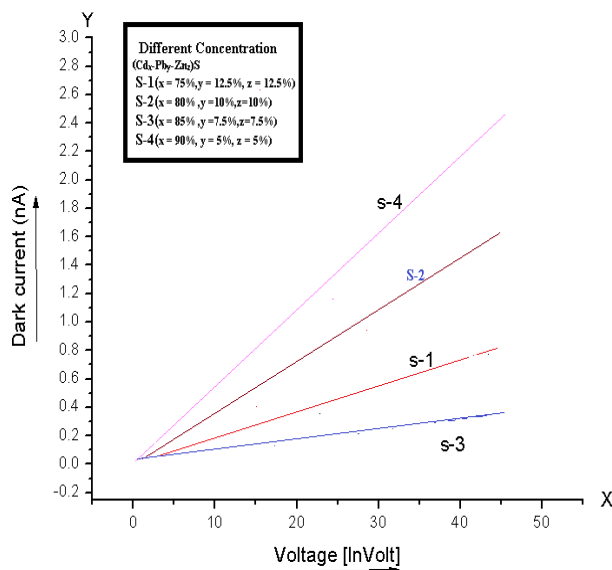


Figure 2: Dark current vs. voltage [1].

**Study of dark current:** A study of the fluctuation in sample dark current v/s voltage is shown in Figure 2. These figures illustrate a little variation in dark current when there is no external light source at various concentrations. According to Figure 2, DC is the least for sample No. 3 and the maximum for sample No. 4 [8].

### 3. Results and discussion

#### 3.1 Structural analysis and surface morphology

Figure 3 shows the XRD pattern of the  $(\text{Cd}_x\text{-Pb}_y\text{-Zn}_z)\text{S}$  photoconductive material. This pattern demonstrates how many notable peaks reach their respective planes. Diffraction lines are assigned by comparing them to ICSD data. The XRD pattern's peaks all match up with typical ICSD data for CdS, ZnS, and PbS. The Debye-Scherrer formula was implemented to estimate the average size of crystallites.

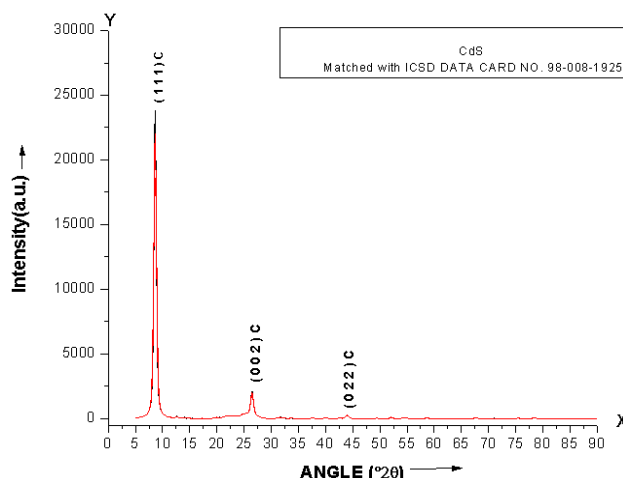


Figure 3: XRD patterns of the CdS thin films.

$$D = 0.94\lambda/\beta\cos \theta \quad (1)$$

where  $\lambda$  is wavelength of the x-ray = 1.5406 Å,  $\beta$  is the FWHM of (111)C peaks, and  $\theta$  is the Bragg angle.

The range of crystallite sizes of grain has been found to be 5.717 nm at the highest peaks. In addition to determining

characteristics like the lattice interval, lattice constant, and Miller indices, XRD is used to analyse the samples. Sharp peaks suggest a polycrystalline structure for the produced films. The overall crystal is composed of many atomic layers in cubic phases.

The materials used to create the film that was deposited matched the information on ICSD data card number 98-008-1925 with stick pattern diagram Figure 4 of CdS, which verified the film's creation having a cubic structure. The crystal structure is cubic at the plane [111] of space group (F-4 3 m) and space group number 216 [9].

Figure 3 shows the stick pattern of matched XRD data, and table number 1 explains the details of the XRD pattern on which PbS has a cubic structure with space groups (F m -3 m) and space group number 225 and matched the information on ICSD data card number 98-064-8452 with stick pattern diagram Figure 5 [10].

Similarly, ZnS belongs to space group (F -4 3 m) and space group number 216 with a cubic structure and matched the information on ICSD data card number 98-016-8377 with stick pattern diagram Figure 6 [11].

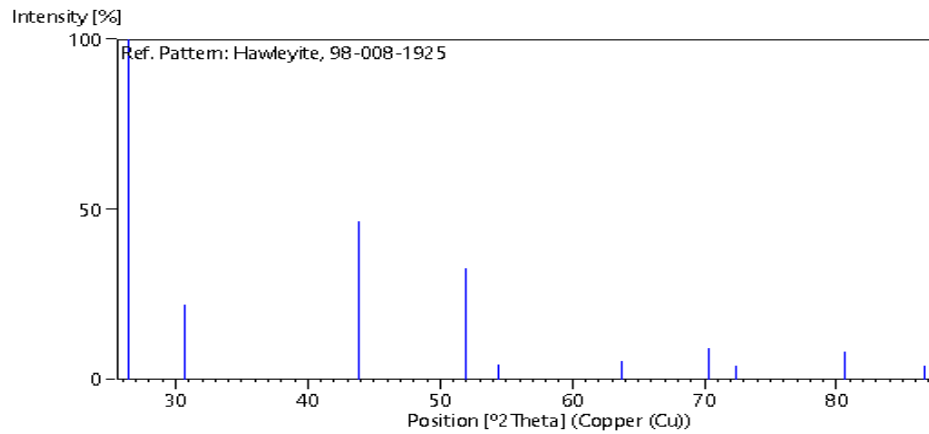


Figure 4: Stick patterns of the CdS thin films.

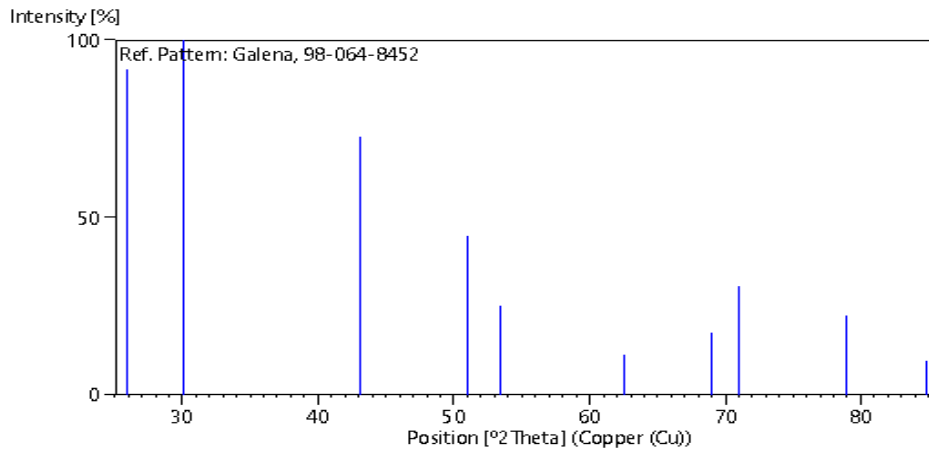


Figure 5: Stick patterns of the PbS thin films.

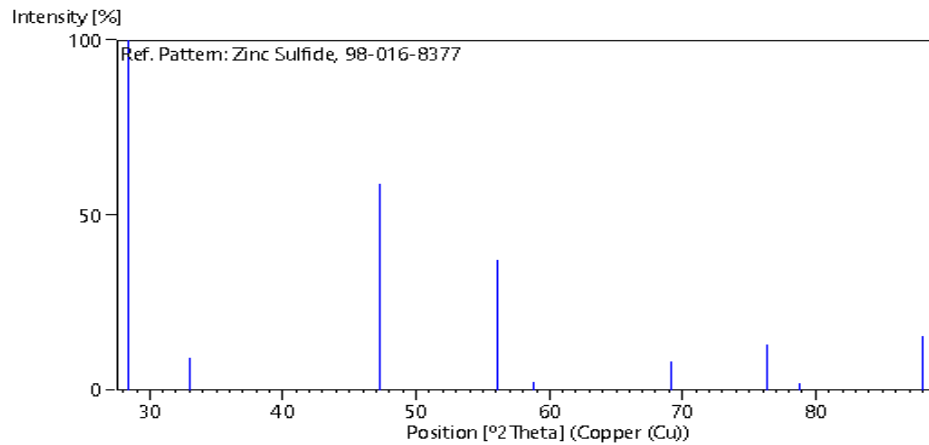
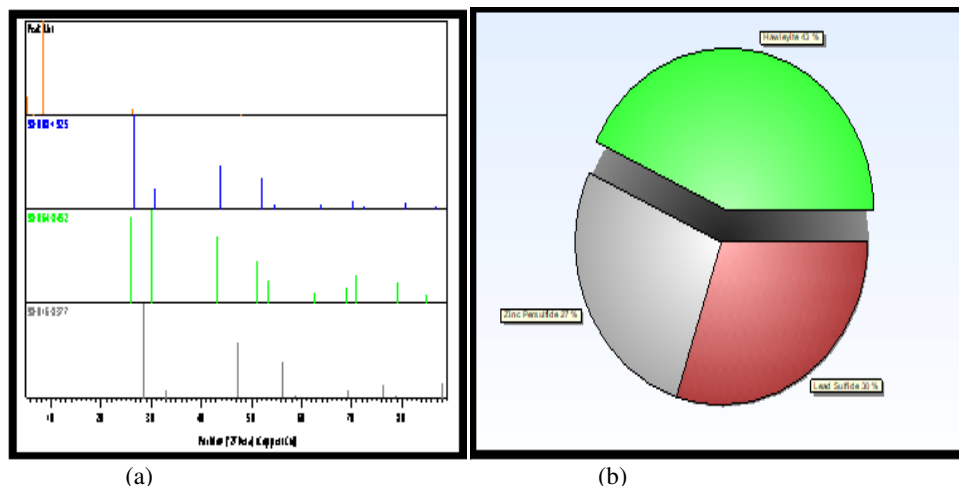


Figure 6: Stick patterns of the ZnS thin films.



**Figure 7:** (a) Stick patterns of the  $(\text{Cd}_x\text{-Pb}_y\text{-Zn}_z)\text{S}$ , (b) Quantification of compound in  $(\text{Cd}_x\text{-Pb}_y\text{-Zn}_z)\text{S}$  thin films.

Figure 7(a) shows the stick patterns of the  $(\text{Cd}_x\text{-Pb}_y\text{-Zn}_z)\text{S}$  of whole films and Figure 7(b) shows the percentage quantification of compound in thin films, where the CdS compound is composed of 43% haweylite structure and 30% of

PbS and 27% of ZnS both are in the cubic compound. Table 2 illustrates the pattern list of  $(\text{Cd}_x\text{-Pb}_y\text{-Zn}_z)\text{S}$  film, in which CdS, ZnS and PbS includes in the XRD pattern and stick patterns and verifies present of this compound.

**Table 1:** The matched data of  $(\text{Cd}_x\text{-Pb}_y\text{-Zn}_z)\text{S}$  with the ICSD Data Card Number

Compound name	Space group	Lattice constant	ICSD data card No.
CdS (cubic)	F -4 3 m	$a = b = c = 5.8300 \text{ \AA}$	98-008-1925
PbS (cubic)	F m -3 m	$a = b = c = 5.9340 \text{ \AA}$	98-064-8452
ZnS (cubic)	F -4 3 m	$a = b = c = 5.4300 \text{ \AA}$	98-016-8377

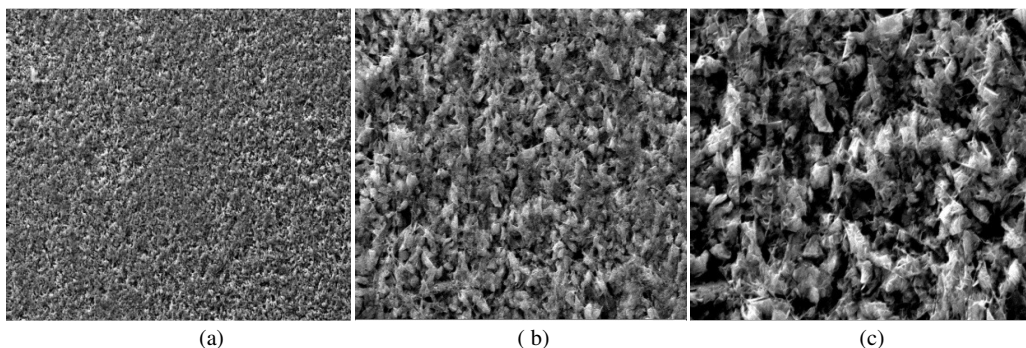
**Table 2:** Pattern List

Ref. code	Score	Compound name	Scale factor	Chemical formula
98-008-1925	57	Hawleyite	0.048	$\text{Cd}_1\text{S}_1$
98-064-8452	26	Galena	0.013	$\text{Pb}_1\text{S}_1$
98-016-8377	27	Zinc Sulfide	0.006	$\text{S}_1\text{Zn}_1$

### 3.2 Structural morphology and elemental study

Scanning electron microscopy (SEM) was used to investigate the surface morphology of as-deposited  $(\text{Cd}_x\text{-Pb}_y\text{-Zn}_z)\text{S}$  thin films [12]. Figure 8 shows the SEM micrograph of an as-deposited  $(\text{Cd}_x\text{-Pb}_y\text{-Zn}_z)\text{S}$  thin film. The deposited thin film is homogeneous, with a few isolated clusters visible in the scanning electron micrographs. These few well-defined high-density development regions (clusters) may be attributed to local heterogeneity in growth conditions.

The chemical homogeneity of the films was assessed using EDAX. The EDAX spectra were acquired at various spots throughout the film. The typical EDAX spectrum of the as-deposited thin film appears to be displayed in Figure 9. The different quantities of cadmium, lead, and zinc X-ray counts at different sites revealed that the composition of thin film was nonstoichiometric in nature.



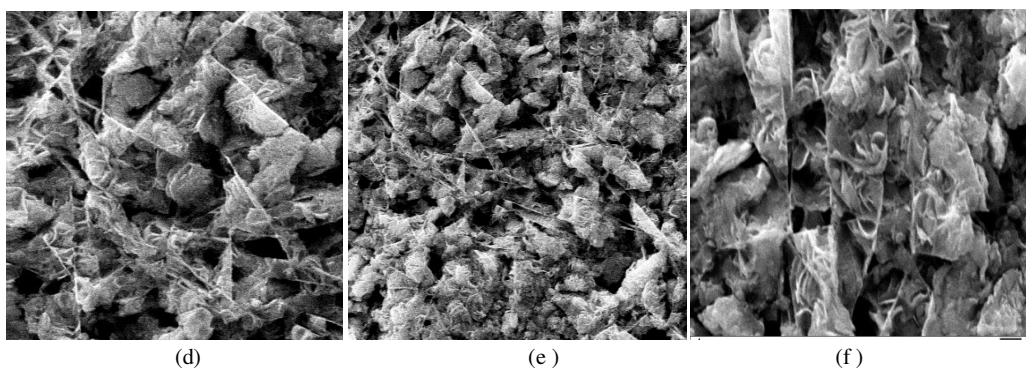


Figure 8: SEM micrographs of  $(Cd_x-Pb_y-Zn_z)S$  at different magnifications [1KX, 5KX, 10KX, 15KX, 20KX, 30KX].

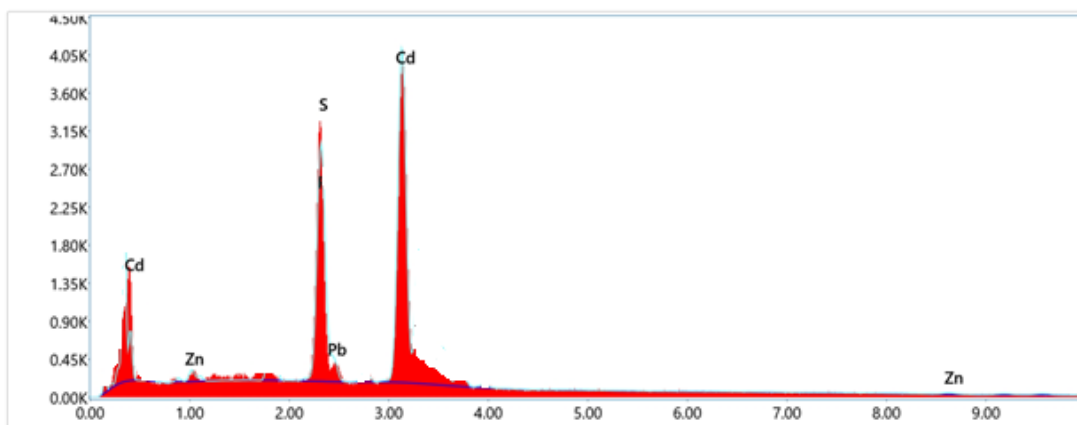


Figure 9: EDAX image of  $(Cd_x-Pb_y-Zn_z)S$ .

Table 3: Quantitative elemental analysis of as-deposited  $(Cd_x-Pb_y-Zn_z)S$  thin films

Element	Link type	Wt %	Atomic %
Zn	K series	3.49	3.44
Cd	L series	93.65	94.37
Pb	M series	2.86	2.19
Total		100	100

### 3.3 Fourier-Transform Infrared Spectroscopy (FTIR)

A thin film of  $(Cd_x-Pb_y-Zn_z)S$  as deposited appears by different FTIR peaks in Figure 10. The FTIR spectrum has a peak at  $3350\text{ cm}^{-1}$  due to cadmium sulphide and a peak at  $3350\text{ cm}^{-1}$  due to free O-H group; a peak at  $1700\text{ cm}^{-1}$  due to the

presence of the hydroxyl group of the water C-H bond; a peak at  $1450\text{ cm}^{-1}$  due to the S-O bond; and a peak at  $1000\text{ cm}^{-1}$  due to the S-S bond. The Cd-S bond is the reason for the peak at  $650\text{ cm}^{-1}$  [13].

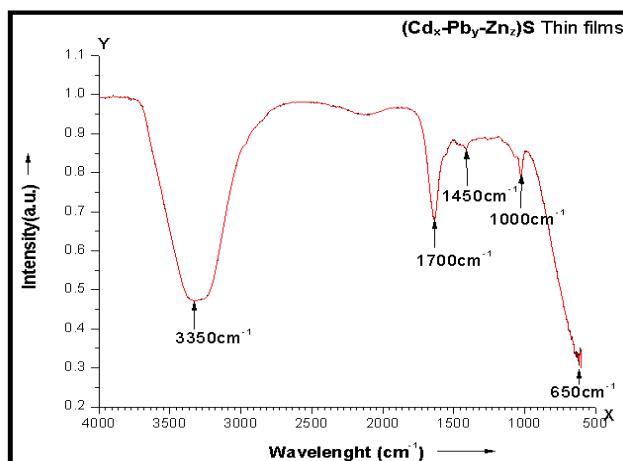


Figure 10: The FTIR spectrum of the  $(Cd_x-Pb_y-Zn_z)S$  thin film.



**Table 4:** Interpretation of the peaks obtained by the FTIR spectra of the synthesized (Cd<sub>x</sub>-Pb<sub>y</sub>-Zn<sub>z</sub>)S thin film [13].

Peak	Region	Intensity	Interpretation
a	400-480	Sharp and strong	Cd-S bond stretching (CdS nanoparticles)
b	650-850	Small and weak	S-S-S bending or C-H stretching (crystal s-s-s bond or acetone)
c	1060-1120	Broad and small	C-O or S-O (acetone or sulphate)
d	1380-1640	Sharp and small	C-H bending of CH <sub>3</sub> (Acetone)
e	3140-3460	Sharp and small	Intermolecular H-bonds (Lattice water)

## 5. Conclusions

The photoconductive (Cd<sub>x</sub>-Pb<sub>y</sub>-Zn<sub>z</sub>)S thin film was fabricated using a cost-effective chemical bath deposition technique on a glass substrate. Photocurrent for sample number No. 3 is  $4.75 \times 10^{-6}$  maximum and gain is also  $47 \times 10^6$  maximum. The X-ray analysis revealed a cubic structure. From the XRD result, the particle size at the highest peak is 5.717 nm. The SEM micrograph gives the spherical-type structure, and EDAX confirms that all elements used in the deposition of thin films are present in our prepared films in non-stoichiometric form.

## Acknowledgements

We would like to thank the Metallurgy and Metrology Department (NIT Raipur), SOS Department of Physics (Pt. R. S. U. Raipur), and Dr. M. Chopkar (Asst. Professor, NIT Raipur). Department of Chemistry, Govt. V.Y.T.P.G. Autonomous College, Durg (C.G.), India, Department of Physics, Govt. V.Y.T.P.G. Autonomous College, Durg (C.G.), India, IIT Bhilai C.G., SAF Coachi for encouragement and providing facilities to carry out work smoothly.

## Author contributions

A special thanks to my guide, Dr. Neelam Shukla [Asst. Prof.] Department of Physics, Kalyan P.G. College, Bhilai, Durg (C.G.), for encouraging the continuation of the work in India, and my co-guide, Dr. Purna Bose [HOD] Department of Physics, Govt. V.Y.T.P.G. Autonomous College, Durg (C.G.), for supporting practical works and encouragement.

## References

- [1] C.S. Verma, N. Shukla, P. Bose, A review on chemical bath deposition mediated synthesis of binary/ternary photoconductive metal sulfide thin films, *ECS Trans.* **107** (2022) 19647.
- [2] G. Murugadoss, R. Jayavel, R. Thangamuthu, M. Rajesh Kumar, PbO/CdO/ZnO and PbS/CdS/ZnS nanocomposites: Studies on optical, electrochemical and thermal properties, *J. Luminescence* **170** (2016) 78-89.
- [3] R. Zellagui, H. Dehdouh, M. Adnane, M. Saeed Akhtar, M.A. Saeed, Cd<sub>x</sub>Zn<sub>1-x</sub>S thin films deposited by Chemical Bath Deposition (CBD) method, *Optik* **207** (2020) 164377.
- [4] A. Oudhia, N. Shukla, P. Bose, R. Lalwani, A. Choudhary, Effect of various synthesis protocols on doping profile of ZnO:Eu nanowires, *Nano-Str. Nano- Obj.* **7** (2016) 69-74.
- [5] S. Thirumavalavan, K. Mani, S. Suresh Sagadevan, Studies on Hall effect and dc conductivity measurements of semiconductor thin films prepared by chemical bath deposition (CBD) method, *J. Nano Electron. Phys.* **07** (2015) 04024.
- [6] S. Thirumavalavan, K. Mani, S. Sagadevan, Investigations on the photoconductivity studies of ZnSe, ZnS and PbS thin films, *Sci. Res. Essays* **10** (2015) 362-366.
- [7] D. Rodic, V. Spasojevic, A. Bajorek, P. Onnerud, Similarity of structure properties of Hg<sub>1-x</sub>Mn<sub>x</sub>S and Cd<sub>1-x</sub>Mn<sub>x</sub>S (structure properties of HgMnS and CdMnS), *J. Magnetism Magnetic Mater.* **152** (1996) 159-164.
- [8] C.S. Verma, N. Shukla, P. Bose, Electrical and structural properties of chemically deposited photoconducting films, *J. Phys.: Conf. Series* **2576** (2023) 012009.
- [9] D. Langner, H. Krebs, A. Zeitschrift fuer, Über Struktur und Eigenschaften der Halbmetalle. XVI. Mischkristallsysteme zwischen halbleitenden Chalkogeniden der vierten Hauptgruppe. II, *Allgemeine Chemie* **334** (1964) 37-49.
- [10] E. Deligoz, K. Colakoglu, N. Korozlu, First-principles study of structural, elastic, lattice dynamical and thermodynamical properties of GdX, *Physica Stat. Sol. Sectio B: Basic Res.* **247** (2010) 1214-1219.
- [11] K.L. Narayanan, Chemical bath deposition of CdS thin films and their partial conversion to CdO on annealing, *Bull. Mater. Sci.* **20** (1997) 287-295.
- [12] R. Hepzi Pramila Devamani, R. Kiruthika, P. Mahadevi, S. Sagithapriya, Synthesis and characterization of cadmium sulfide nanoparticles, *IJISSET – Int. J. Innov. Sci. Eng. Technol.* **4** (2017) 2348-7968.
- [13] N. Qutub, S. Sabir, Optical, thermal and structural properties of CdS quantum dots synthesized by a simple chemical route, *Int. J. Nanosci. Nanotechnol.* **8** (2012) 111-120.

**Publisher's Note:** Research Plateau Publishers stays neutral with regard to jurisdictional claims in published maps and institutional affiliations.